Revista Geográfica de Chile Terra Australis, Vol.61, No. 1 (2025) 15-38 ISSN 0719-9562
https://doi.org/10.23854/07199562.2025611.gutierrez

PRONÓSTICO DE INUNDACIONES EN CUENCAS DE RESPUESTA RÁPIDA: UN ESTUDIO DE CASO DE LA MICROCUENCA YACUPUGRO DE LAS LADERAS DEL VOLCÁN PICHINCHA EN QUITO, ECUADOR

FLOOD FORECASTING IN RAPID RESPONSE THE BASINS – A CASE STUDY OF THE YACUPUGRO MICRO-BASIN OF THE SLOPES OF PICHINCHA VOLCANO IN QUITO, ECUADOR

Carlos Aníbal Gutiérrez-Caiza[1], Víctor Espinoza-Romero[2] and Theofilos Toulkeridis[3,4*]

RESUMEN

El presente estudio presenta una metodología de análisis de inundaciones aplicable a cuencas urbanas con tiempos de concentración menores a 20 minutos, siendo el caso de la microcuenca Yacupugro en Ecuador, la cual presenta un tiempo de concentración de 15,22 minutos, una pendiente de 31%, ocasionando inundaciones violentas. El mes más lluvioso es diciembre, seguido de febrero, marzo, noviembre, abril y enero en orden según el número de frecuencia y probabilidad de ocurrencia de inundaciones. Al no existir datos sobre caudales medidos en la microcuenca, se utilizaron métodos hidrometeorológicos indirectos basados en precipitaciones máximas en 24 horas y curvas de intensidad, duración y frecuencia – IDF, permitiendo comparar resultados. En este trabajo, la metodología utilizada incluyó el análisis de hietogramas mediante el método de bloques alternados, de los caudales máximos de avenida con el modelo lluvia-escorrentía, además de la aplicación de un sistema de pronóstico de inundaciones de microcuencas de respuesta rápida. La Empresa Pública Metropolitana de Agua Potable y Saneamiento de Quito (EPMAPS) ha construido un canal trapezoidal (h=1,70 m, b=3,80 m y m=1,5) que recoge agua de las microcuencas de los ríos Yacupugro y Sin nombre (S/N), conduce a un reservorio ubicado en la microcuenca San Isidro ubicada a su suroeste, para luego depositarla en el alcantarillado de la EPMAPS. Fue modelado con un caudal total de 7,60 m3/s, correspondiente a una precipitación de 85,3 mm y un periodo de retorno de 100 años. Así, se observó que el canal opera a su máxima capacidad y el reservorio con sus estructuras aplaca este tipo de avenidas sin desbordarse, cumpliendo su función, siempre y cuando dichas estructuras se encuentren limpias. La alerta se basó en el umbral de precipitación previa (agua acumulada en el suelo durante los últimos 10, 7, 5 y 3 días), considerando el tipo de suelo para alcanzar la capacidad de campo llegando a una profundidad de un metro, necesitando absorber al menos 129 mm de agua. Con esto fue posible concluir que el sistema de pronóstico es capaz de iniciar un aviso anticipado si la precipitación estimada entre 3 a 7 días supera los 129 mm. De esta manera, se puede pronosticar con bastante anticipación al momento de concentración.

Palabras clave: microcuencas urbanas, tiempos de concentración, pronóstico de inundaciones, período de retorno, precipitación antecedente

ABSTRACT

The current study presents a flood analysis methodology applicable to urban basins with concentration times less than 20 minutes, being the case of the Yacupugro micro-basin in Ecuador, which has a concentration time of 15.22 minutes, a slope of 31%, causing violent floods. The rainiest month is December, followed by February, March, November, April and January in order according to the number of frequency and probability of occurrence of floods. Since there was a lack of data on flows measured in the micro-basin, indirect hydrometeorological methods based on maximum rainfall in 24 hours and intensity, duration and frequency curves - IDF were used, allowing to compare results. Hereby, the methodology used included the analysis of hyetographs using the alternating block method, of the maximum flood flows with the rain-runoff model, besides the application of a rapid response micro-basin flood forecasting system. The Metropolitan Public Company of Potable Water and Sanitation of Quito (EPMAPS) has built a trapezoidal canal (h = 1.70 m, b = 3.80 m and m = 1.5) that collects water from the Yacupugro and Unnamed river (S/N) micro-basins, leads to a reservoir located in the San Isidro micro-basin located to its southwest of, and then deposits it in the EPMAPS sewer system. It was modeled with a total flow of 7.60 m^3 / s, corresponding to a rainfall of 85.3 mm and a return period of 100 years. Thus, it was observed that the canal operates at its maximum capacity and the reservoir with its structures plates this type of floods without overflowing, fulfilling its function, if these structures are clean. The alert was based on the threshold of previous precipitation (water accumulated in the soil during the last 10, 7, 5 and 3 days), considering the type of soil to reach the field capacity reaching a depth of one meter, needing to absorb at least 129 mm of water. With this it was possible to conclude that the forecast system can start with an advance warning if the antecedent rainfall in 3 to 7 days once it exceeds 129 mm. Thus, it can be forecast well in advance of the time of concentration.

Keywords: urban micro-basins, concentration times, flood forecast, return period, antecedent precipitation

[1] Magister en gerencia de proyectos educativos y sociales, Grupo de Investigación de Recursos Hídricos y Acuáticos, Universidad Regional Amazónica Ikiam, Parroquia Muyuna.
[2]Magister en gestión de proyectos, Grupo de Investigación de Recursos Hídricos y Acuáticos, Universidad Regional Amazónica Ikiam, Parroquia Muyuna.
[3]School of Geology, Aristotle University of Thessaloniki, 54124 Thessaloniki, Greece
[4]Universidad de Especialidades Turísticas UDET, Quito, Ecuador
Corresponding author: ttoulke@geo.auth.gr

1. INTRODUCTION

The growth of the world's population, particularly in developing countries, threatens protected areas due to urbanization and migration (McDonald et al., 2008; Wittemyer et al., 2008; Raleigh, 2011). This results in impacts on terrestrial and aquatic ecosystems and the population itself, causing floods, diseases, disasters, economic losses and quality of life, due to the lack of control of urban space (Singh & Singh, 2017; Sivakumar, 2011; Moore et al., 2003; Sekovski et al., 2012). This subsequently, may produce direct effects on water infrastructure, such as supply, sanitation, urban drainage and riverine flooding and solid waste (Sarker et al., 2021; Mokuolu et al., 2022; Dibaba, 2018; Koop & van Leeuwen, 2017; Poma et al., 2022; Poma et al., 2025). Globally, between 1970 and 2024, more than 12,000 disasters caused by meteorological, climatic and water-related hazards were reported, which caused approximately two million deaths (Lee et al., 2020; Veenema et al., 2017; Grayman, 2011; Cann et al., 2013; Gopalakrishnan, 2013; Zou et al., 2023; Moncayo-Galárraga et al., 2022; Sandoval Erazo et al., 2021). Storms and floods accounted for 79% of all such disasters and were responsible for 54% of deaths (Jonkman & Kelman, 2005; Jonkman, 2005; Hamidifar & Nones, 2021; Liu et al., 2023; Liu et al., 2022). In Latin America and the Caribbean, 71% of the records of intensive and extensive manifestations of the risks were triggered by hydrometeorological phenomena, observing, for every 100 thousand inhabitants, an increase of 300% of affected people and 600% of damaged houses (Pinos & Quesada-Román, 2021; de Moraes, 2021; Marengo et al., 2022; Santos et al., 2023).

Due to the constellation of different tectonic plates, Ecuador, along the northwestern South American continent, is prone to a variety of geological and hydrometereological hazards as well as climate change (Lonsdale, 1978; Jaillard et al., 2000; Daly, 1989; Poveda et al., 2020; Pabón-Caicedo et al., 2020; Macías et al., 2024; Reyes Pozo et al., 2020; Castelo et al., 2018; Toulkeridis et al., 2020; Macías et al., 2025). Nonetheless, the atmospheric and climatic processes are especially pronounced which trigger frequently the El Niño and La Niña phenomena, resulting to catastrophic floodings besides the regular floodings within the annual rainy seasons (Rosales-Rueda, 2018; Bendix et al., 2011; Hederra, 1987; Pinos & Timbe, 2020; Mato & Toulkeridis, 2017). Based on these occurrences, flooding and associated landslides, count to the most lethal hazards within Ecuador (Alonso-Pandavenes et al., 2024; Pinos & Timbe, 2020; Orejuela & Toulkeridis, 2020, April; Castelo et al., 2018; Salcedo et al., 2018; Poma et al., 2021). Hereby, the National Secretariat for Risk Management (SNGR) in Ecuador in its database indicates that most of the deadliest and destructive floodings have occurred in the highlands where thousands of hectares of lost crops have been counted, besides the destruction of tens of thousands of homes, including hundreds of educational canters and strategic infrastructure, which economic damage surpasses billions of USD (Rojas et al., 2022; Bucherie et al., 2022; Alonso-Pandavenes et al., 2024; Oliveira et al., 2023).

The Metropolitan District of Quito (DMQ), capital of Ecuador is located in the province of Pichincha, Guayllabamba River basin is one of the main economic, productive, industrial, cultural and sports centers of Ecuador. In recent decades it has experienced accelerated processes of informal urban growth in sites considered high threat located on the slopes of the Pichincha near the margins of its micro-basins, developing unsafe conditions for the population, their goods, means of production and infrastructure in general (Salcedo et al., 2022; Albán-Campaña et al., 2021; Toulkeridis et al., 2016; Toulkeridis et al., 2015). Flooding in Quito intersects with urban growth and hazardous areas, affecting designated green spaces, which could serve as emergency shelter but are at risk due to urbanization and environmental hazards (Mejia et al., 2023; Trizio et al., 2022; Domínguez-Castro et al., 2018; Velez et al., 2022).

In past, a variety of mudflows affected the city. Some prominent cases were recorded in “La Gasga” in 1975, 2022 and 2024 (Brachhi et al., 2020; Troncoso et al., 2024; Poma et al., 2024). One of the most recently, the 2022 mudflow in Quito was exacerbated by urban development and inadequate drainage management, highlighting vulnerabilities on the slopes of the Pichincha during episodes of heavy rainfall (Troncoso et al., 2024). Mudflows in Quito, particularly on the slopes of Pichincha, are influenced by rainfall, topography and urban infrastructure, significantly affecting urban areas and disaster risk management (Troncoso et al. 2024). Hereby, flooding in the Metropolitan District of Quito is mainly caused by urbanization and saturated contributing areas on

the slopes of Pichincha, exacerbated during heavy rainfall events (Valdivieso-García et al., 2024; Pillosu et al., 2024; Loor, 2024).

Based on this reality, in the 1970s, the Municipal Sewerage Company (EMA) constructed works to mitigate the impact of floods and avalanches in populated areas on the eastern slopes of the Pichincha Volcano (Sarmiento, 2009; Marrero et al., 2023). These works consisted of containment dams within the channels of the micro-basins and channels for the transfer of floodwaters in micro-basins whose collectors in urban areas had low hydraulic capacity to other micro-basins with collectors that could supply the reception of significant flows of floodwater and mud during the rainy season (Puente-Sotomayor et al., 2021; Vallejo et al., 2018). A technical report reported in March 1985 (Camp Dresser & McKee International Inc 1985), developed studies in the fields of hydrology, hydraulics and geology in the Yacupugro micro-basin with the purpose of proposing complementary measures to attenuate or reduce the impacts of avalanches, focused on controlling erosion on the slopes of the micro-basin (Peltre, 1989).

Flood control works on the slopes of the Pichincha are aimed at mitigating landslides and flooding, incorporating protective forests to prevent erosion and control urbanization in dangerous areas. However, on March 22, 2019, the last major avalanche occurred in the Yacupugro micro-basin, due to the overflow caused by the (informal) modification of the structure of the transfer channel to the Yacupugro micro-basin, blockage of the micro-basin due to lack of maintenance and poor community management of certain residents who dump waste into the micro-basin, which reduced its hydraulic section (Toapanta et al., 2020). This flow moved along Manuel Valdivieso Street and secondary streets, to Av. Mariscal Sucre, affecting several homes, vehicles, belongings, damage to the roads, which forced people to remain within their homes for three days, among others in the Osorio Neighborhood, neighboring neighborhoods and surrounding condominiums such as the Caminos del Pichincha.

This gap in the literature is due in part to the lack of specific models for small, fast-response urban watersheds, such as the Yacupugro microwatershed, where rapid stormwater runoff can generate extreme flows in very short periods of time. Most existing models, such as HEC-HMS and the SCS method, have been adapted from studies conducted in larger watersheds and, although useful, have limitations when applied to urban watersheds with such specific topographic and land-use characteristics.

The current study proposes a new methodology for flood forecasting in rapid-response urban microwatersheds, specifically for the Yacupugro microwatershed. The novelty of this work lies in the integration of indirect hydrological tools, such as hyetographs generated from IDF curves and 24-hour maximum rainfall, with the use of the HEC-HMS model to simulate runoff. Furthermore, the study introduces early warning thresholds based on antecedent rainfall, an innovative approach that allows warnings to be issued sufficiently in advance to mitigate the risk of flash floods. Through this methodology, it is hoped to contribute to the development of early warning systems adapted to rapid-response urban watersheds, providing a useful tool for flood risk management in highly vulnerable areas.

Therefore, the predominant objective of the current research has been to predict floods in rapid response basins using a conceptual model based on previous soil moisture and observed precipitation. This has been realized by evaluating in detail the physical-morphometric characteristics of the studied basin and its corresponding rainfall regime with the analysis of hyetographs using the alternating block method. This may allow to alert the vulnerable population located in the lower part of the micro-basin to evacuate in time for eventual future uprising flooding. Furthermore, this study is distinguished by its focus on the hydrological modeling of rapid-response urban microwatersheds, an area underexplored in the scientific literature and provides a novel tool that can be applied to other urban areas with similar characteristics. The present study also paves the way for future research addressing real-time model calibration and the incorporation of remote sensing and weather radar data.

2. METHODOLOGY

2.1. Location and general description of the micro-basin

The Yacupugro micro-basin is one of the 85 micro-basins on the slopes of the active Pichincha

Volcanic Complex (Toulkeridis & Zach, 2017). It originates in the Pichincha volcano at an altitude of 3,960 meters above sea level (m a.s.l.). It is an elongated micro-basin that runs east-west up to an altitude of 2,920 m a.s.l. It is 3.40 km long and has an elevation difference of 1,040 meters at its lowest point. Its average slope is 31%. Heavy rains produce torrential flows of water and mud due to the high erodibility of its slopes. The slopes of which on both margins are as high as 90°. The western margin produces most landslides due to its steep slopes (Figure 1).

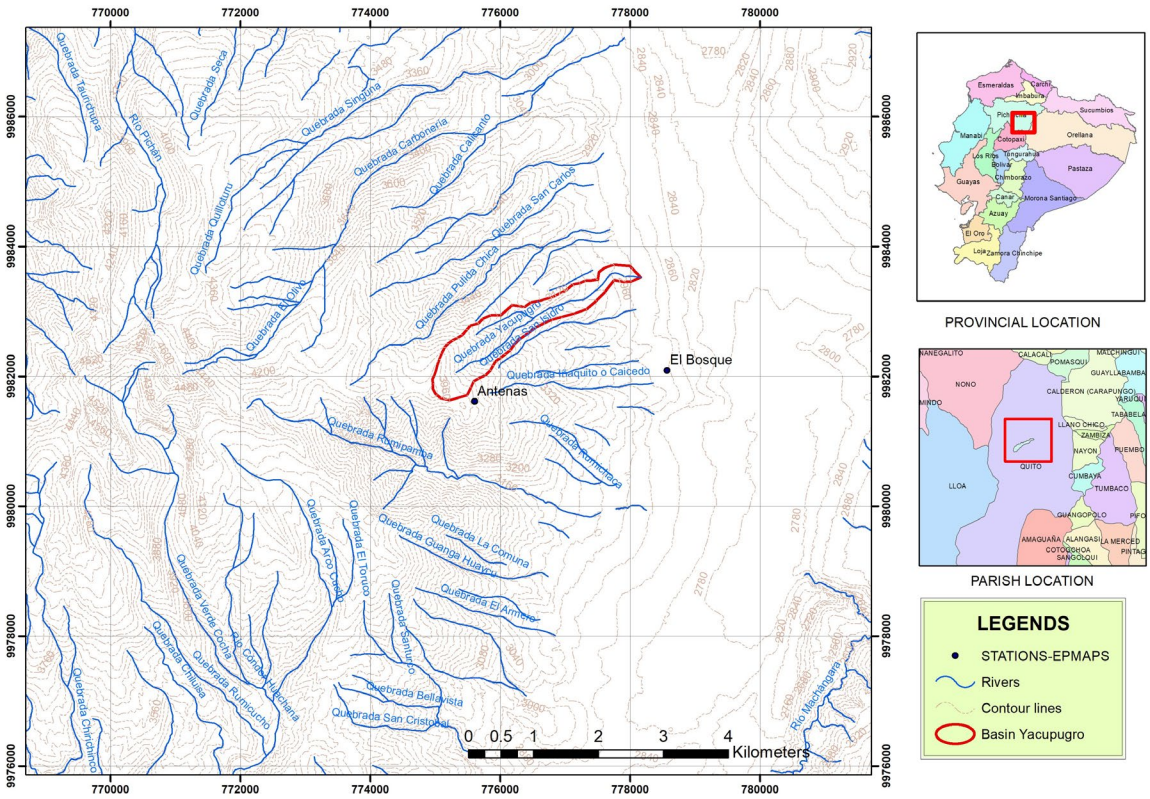

Figure. 1. The geographic location of our research area within Ecuador (upper right), being close to the city of Quito (central right). Main frame illustrates the topographic area of the Yacupugro micro-basin and the corresponding meteorological stations. The study area is marked in red.

The physical-morphometric characteristics of a basin, including shape, relief and vegetation, influence the spatial variation of the hydrological regime (Sahu et al., 2024; Silva et al., 2022). These data provide the possibility of knowing the variation in space of the hydrological regime and to obtain these parameters, the topographic map of Quito the Military Geographical Institute (IGM) was used. On this, the micro-basin was drawn, and several morphometric parameters of the basin were obtained, including topographic and geomorphometric aspects, using Arcgis 10.4 (Bajirao, 2021). Furthermore, the land use in this area is focused on livestock, although on a small scale it makes use of the moor vegetation, which is composed of grasslands, natural pastures and other species characteristic of this plant formation. Next to it, natural forests and forest plantations are developed, composed of primarily of eucalyptus (*Eucaliptus globulus*), isolated cypress trees (*Pinus radiata*) and acacias (*Acacia mollisima*). Plantations that were established as protective forests in the lower and central part of the micro-basin. Artificial pastures of kikuyu (*Pennisetum clandestinum*) can also be found associated with creeping legumes, especially white clover (*Trifolium repens*), which are located in the watersheds with undulating relief. To obtain the land use map of the Yacupugro micro-basin, the available information of the IGM was used, with a scale of 1:100,000, using Arcgis 10.4 (Bajirao, 2021).

2.2. Rainfall regime

In the study area there are two meteorological stations close to the micro-basin (Figure 1), with daily, monthly and annual rainfall data, whose characteristics are listed in Table 1. To determine the rainfall regime or pluviometric behavior of the Yacupugro micro-basin, the Antenas - P11 meteorological station was used, which is the closest (Figure 1). According to the Thiessen method, the estimated values over geographic areas weighted according to proximity, proving to be efficient in estimating expected values with a confidence interval of 95% (Watson et al., 2022). It has a period of 23 years of information (2000-2022), being the most representative due to its location, with which the analysis of the pluviometric regime is performed.

Table 1. Characteristics of meteorological stations near the study area.

CODE	NAME	COORDINATES N	COORDINATES E	ALTITUDE m a.s.l.	STATISTICS YEARS
P11	Antenas	9981632	775602	3800	2000-2022
P70	CC El Bosque	9982111	778569	2903	2016 -2022

It was indicated that the daily rainfall is the total amount of rainwater during a day, ranging between 7:00 on the current day and 7:00 on the following day. For the analysis of daily rainfall, information from the Antenas-P11 meteorological station was used (Figure 1 and Table 1), observing maximum annual values of daily rainfall and the dates on which these maximums have occurred.

Table 2. Annual maximum daily precipitation (Station: Antenas, P11), 2000-2022.

DATE	28/12/00	15/3/01	21/3/02	27/2/03	25/11/04	15/2/05	19/12/06	19/4/07
P max. (mm)	45.8	36.2	40.0	33.5	32.7	37.5	**49.2**	35.7
DATE	21/2/08	28/3/09	15/11/10	30/7/11	25/12/12	31/12/13	8/1/14	31/10/15
P max. (mm)	44.8	45.1	42.8	31.5	36.9	35.6	34.7	35.4
DATE	13/01/201	2/12/17	4/4/18	31/12/19	20/11/20	31/5/21		
P max. (mm)	28.0	48.7	45.4	**68.2**	**52.7**	45.9		

To determine a theoretical frequency distribution to which the data of the series of maximum annual daily rainfall corresponding to the total number of years recorded at the meteorological station fit, a statistical analysis of the same was conducted. The Log Pearson Type III, Gumbel and Log Normal methods were used for the analysis of flood frequency. Log Pearson Type III indicated the best performance with a correlation coefficient of 0.93 (Troncoso et al., 2024). The simplest procedure for frequency analysis consists of using the frequency equation proposed by (Chow, 1953; Guo, 2022):

$$x = \bar{x} + S * Kt \quad (1)$$

Where, x = maximum rainfall value estimated for a return period – Tr (mm), $\bar{x}$ = arithmetic average of the series of observed values (mm), S = standard deviation of the series of observed values (mm), Kt = frequency factor (dimensionless) that depends on the type of distribution, return period and number of record data.

It is necessary to clarify between daily rainfall and maximum rainfall in 24 hours, since they are not necessarily the same (Schreider et al., 2000; Westra et al., 2014; Vidal et al., 2018). Daily rainfall is the rainfall recorded during a day and maximum rainfall in 24 hours is the maximum rainfall recorded during a continuous period of 24 hours. The latter being the most damaging, since it does not allow the soil to decrease its water content and therefore increase its storage capacity. To estimate the maximum rainfall in 24 hours it is necessary to have a pluviograph to later analyze the band and obtain the continuous record and in the area it is not counted. It has been suggested that the magnitude of 24-hour rainfall is approximately 13% greater than the magnitude of daily rainfall (Fattahi & Habibi, 2022). Therefore, knowing the maximum

daily rainfall magnitudes, maximum rainfalls of 24-hour duration can be inferred and subsequently inferred for shorter periods (Watson et al., 2022)

2.3. Analysis of hyetographs using the alternating block method

This method is a simple way to develop a design hyetograph using the Intensity, Duration and Frequency curves and then apply the synthetic unit hydrograph method, using the Soil Conservation Service – SCS method (EMAAP-Q, 2009), and obtain the maximum flood flows for the return periods required in the study. The intensity – duration – frequency curves are obtained, and the way to use these equations considering the following issues (EMAAP-Q, 2009). The DAC-Airport station equation can be used in sectors located north of the airport. It does not say anything about the La Chorrera station equation, which in this case is the one located on the slopes of Pichincha at the height of El Tejar at 3165 m a.s.l., whose height agrees with that of the Yacupugro micro-basin, so the hyetograph was generated based on equation 3 (Watson et al., 2022).

$$DAC - AIRPORT \;\; 0°08\,24,\, 78°29\,06",\, 2794\ m\ \text{a.s.l.},\, I = \{55{,}6656 * T^{0.0922} * [\ln(t+3)]^{4.1647} * (lnT)^{0.0985}\}/t^{1.6567} \quad (2)$$

$$LA\ CHORRERA \;\; 0°12\,06,\, 78°32\,06",\, 3165\ m\ a.s.l.,\, I = \{44.2595 * T^{0.0973} * [ln(t+3)]^{4.4013} * (lnT)^{0.0317}\}/ t^{1.6591} \quad (3)$$

Where: I = Intensity – mm/h, T= Return period – years, t= duration of rainfall – minutes

2.4. Analysis of maximum flood flows - Rain-runoff model

In the Yacupugro micro-basin there is no hydrometric station in operation, so for the present study it was decided to apply indirect hydrometeorological methods (Babu & Kumar, 2024).To transform rainfall into runoff, the HEC-HMS 4.11 hydrometeorological model was used (Verma & Verma, 2023), applying the methodology proposed by the Soil Conservative Service (SCS) (Abraham et al., 2019). To do this, it is necessary to determine the CN curve number which is obtained from the different uses and types of soil. The hydrological groups in the micro-basin correspond to soils A, B and D with their corresponding percentages, antecedent humidity conditions (AMC) of Type II, which is advisable for floods (Chow, 1953; Guo, 2022). For the average case for annual floods, the average conditions existing before the maximum flood occurs in mentioned micro-basins (layer 35 – 50 mm) (Salami et al., 2017; Al-Dughairi, 2023). The transformation model used was the SCS unit hydrograph. It has been mentioned that a study of the unit hydrographs of many large and small rural micro-basins indicates that the lag time is equivalent to 0.6 of the concentration time of the micro-basin.

In order to have a greater reliability in the results, it was also decided to generate flows with precipitations generated through hyetographs applying the method of alternating blocks (Pinheiro et al., 2024) and maximum rainfall of 24 hours, to obtain the corresponding values of maximum flows for return periods of 10, 25, 50 and 100 years for the micro-basin, in the first case applying the hydrological model HEC-HMS 4.11 (Verma & Verma, 2023; Bell & Kar, 1969). In the second case applying the unit hydrograph of the SCS, to compare their results and allow making the best decision (Mendoza et al., 2021).

2.5. Obtaining rainfall-level-flow curves in a channel that intercepts waters

At the coordinates 777264, 9983178 and elevation 3036 m a.s.l., the Metropolitan Public Water and Sanitation Company of Quito (EPMAPS-Q) has built a trapezoidal channel with approximate dimensions of h = 1.70 m, base = 3.80, slope m = 1.5, the same, originates in the S/N micro-basin and passes through the Yacupugro micro-basin collecting its waters until depositing in a small regulation reservoir (figure 2). The cross section raised at the confluence of the micro-basin with the channel subjected to a non-permanent flow according to the centennial storm, reaches its maximum level of approximately 0.31 m, this is without considering the level induced by the flow of sediments and debris which is considerable in the events that occurred in these areas. It is suggested to use at least 1.5 m additional to the water surface, giving a total height of 1.80 m that would be overflowing and surpassing the wall of the canal wall that has a height of 1.70 m.

The trapezoidal channel connects with the reservoir (figure 2) whose dimensions are b= 138.70 m, b= 133.0m, c= 59.40 m and d = 32.00 m and 4.5 m as average depth, located in the micro-micro-basin of

the San Isidro micro-basin (coordinates: 777608, 9983182 and elevation: 3010 m a.s.l.). There, the floods from the two micro-basins (S/N and Yacupugro) are laminated, to then evacuate through a square-shaped bottom drain of dimensions 0.70 mx0.70 m and a circular fixed-lip spillway without gates of dimensions: h = 2.15 m and length: 5.20 m connecting to a trapezoidal channel to the San Isidro micro-basin (figure 2). Thus, reducing the flow rate of the reservoir, the risk of flooding in the sectors located downstream of the Yacupugro micro-basin. The volume of water that the reservoir can store is approximately 27,351.45 m^3.

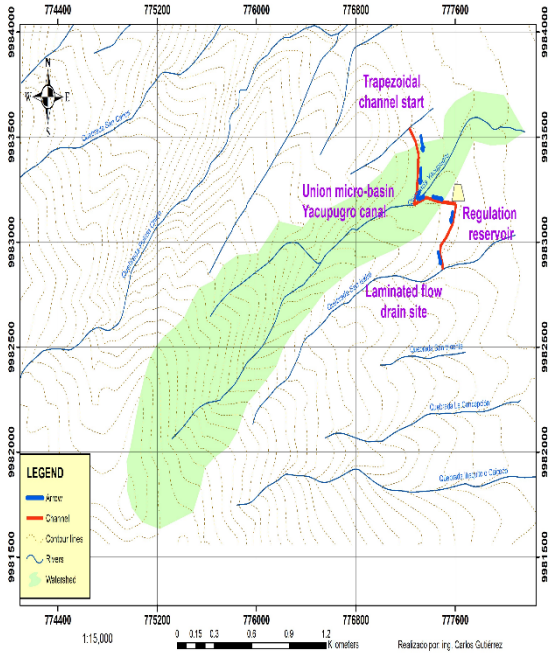

Figure.2. Topographic map of the studied micro-basin, with the associated channel and the regulating reservoir. Note the trapezoidal channel start.

With the data of the reservoir raised in situ, the elevation and area of the reservoir are generated given by the reference elevations 200.00, 200.5, 201.0, 201.5, 202.0, 202.5, 203.0, 203.5, 204.0 and 204.5 in m a.s.l., for an area of 6078.1 m^2 for each of the elevations. The inlet hydrograph to the reservoir is given for the maximum flood of 100 years of recurrence, plus 15% additional flow generated by the S/N micro-basin, giving a total flood flow of 7.60 m^3/s with which the flood lamination modeling is carried out. The reservoir model, included in the HEC – HMS 4.11 program (Verma & Verma, 2023), is suitable for the simulation and development of any configuration of reservoirs or reservoirs and of disposal structures. However, this program assumes that the bottom drains have controlled flow, which is only a function of the water level. If the configuration of the reservoir bottom drains has or is controlled by a backwater effect, downstream of the outlet, this model should not be used, since it does not allow the introduction of the flow conditions after the bottom drain discharge.

2.6. Rapid response micro-basin flood forecasting system and rain levels

The Yacupugro micro-basin has a concentration time of 15.22 minutes, which means that it is a micro-basin with a fast response due to its slope and small area. This type of forecast is based on observed and/or forecast rainfall information – forecast level (Barreto 2017), since reaction times are shorter and the alert time can be increased by performing hydrological modeling using observed rainfall data and those forecast by INAMHI. The alert basically originates based on three thresholds: previous precipitation (amount of water accumulated in the soil during the last 10, 7, 5 and 3 days), forecast precipitation and real-time precipitation. Thresholds are defined for each of these measured elements, which combined with each other provide an alert threshold for the possible onset of rain and in the case of the Yacupugro micro-basin. Due to its characteristics, a rapid response micro-basin forecasting system is proposed, based on the humidity of the micro-basin, observed rainfall data and forecast levels.

The rainfall records of the Antenas – P11 meteorological station of EPMAPS indicate that it had a history of rainfall of 13.3 mm in the previous day, 24.9 mm accumulated in the previous 2 days, 63.2 mm accumulated in the previous 3 days, 107.8 mm accumulated in the previous 4 days, 122.8 mm accumulated in the previous 5 days, 128.5 mm accumulated in the previous 6 days, and 129.5 mm accumulated in the previous 7 days. Therefore, it is necessary to estimate the field capacity of the soil of the micro-basin for this type of information.

2.7. Field Capacity

The Field Capacity is the maximum amount of water that the soil can retain, measured 48 hours after a rain or irrigation, where the water content continues

to decrease as time passes (Assi et al., 2019; Willkofer et al., 2023). To determine if the soil is saturated with the rainfall in the micro-basin, the field capacity is estimated based on the percentages of texture or soil types in the micro-basin (table 3) and the values of useful water content for crops per meter of depth, of the different types of soil according to their field capacity texture minus wilting point (Jankowfsky et al., 2024; Brendel et al., 2020) (table 4).

Table 3. Soil texture percentages, Yacupugro micro-basin.

Soil texture	(Km^2)	(%)	Hydrological classification
Urban	0.111	6.59%	D
Moderately thick	0.569	33.81%	A
Media	1.002	59.60%	B
Total:	**1.682**	**100%**	

Table 4. Average useful water contents for crops per meter of depth, of the different types of soil according to their texture (field capacity minus wilting point (Jankowfsky et al., 2024).

Soil texture	L por m^2
Sandy	62
Sandy loam	103
Clay loam	136
Sandy loam	140
Clay loam	146
Loam	158
Silty clay and silt clay	177
Clayey	187
Silty	192
Fine clayey	208

2.8. Use of local flood records or indirect proxy data

Due to the absence of hydrometric stations in the Yacupugro microbasin, direct calibration of the hydrological model using observed flow records was not possible. Given this limitation, an indirect validation approach was adopted, using available qualitative and quantitative data. This included (1) field observations, visual inspections of the channel during rainfall events, and interviews with local residents and municipal staff were used to identify areas frequently affected by overflows or accumulation of surface flow; (2) the generated flows were compared with the theoretical hydraulic capacity of the existing channel, estimated at 7.60 m^3/s, to verify the consistency of the simulated flows with the observed physical behavior of the system; (3) additionally, the modeled results were verified to correspond to the morphology and slope of the basin, with short concentration times (15.22 min) that justify rapid responses in high-intensity events. This process, while not a substitute for traditional hydrological calibration, allowed to adjust input parameters (such as curve number, runoff coefficient, and delay time) to be adjusted based on expected behavior and local experience, applying criteria of technical validity and hydraulic reasonableness.

In this study, two types of rainfall events were used as input for modeling with HEC-HMS. The first comprised synthetic hyetographs generated from intensity-duration-frequency (IDF) curves, temporally distributed using the alternating block method, in 5-minute increments up to a total duration of 60 minutes. This method allows for a more realistic representation of the concentration of intense rainfall in short periods, typical of rapid-response basins. Furthermore, maximum rainfall over 24 hours, was calculated by fitting probability distributions (Log-Pearson III), which were transformed into streamflows using the SCS unit hydrograph. This approach is widely used in hydrologic design practice due to its simplicity and availability of daily historical records.

The comparison between the two approaches allowed us to evaluate the model's sensitivity to different representations of extreme events and address two complementary objectives, being to capture the real dynamics of short-duration events (hyetographs), and, additionally to ensure a conservative and safe hydraulic design based on absolute maximums (24-hour precipitation).

2.9. Reliability

Due to the lack of direct hydrometric records, indirect hydrological methods were used. The were two approaches used, being first the synthetic hyetographs generated from IDF curves, applied in the HEC-HMS 4.11 model. This method allows for a more detailed representation of the temporal

distribution of rainfall during short-duration events, realistically simulating the rapid response of the basin. This was followe by the use of the Maximum 24-hour rainfall, which was converted into streamflow using the SCS unit hydrograph. This approach is more conservative and widely used in hydraulic design practice due to its simplicity and availability of daily historical data.

A comparison of the two methods allowed for an analysis of the sensitivity of hydrological results to different representations of extreme events. It was observed that, for long return periods (such as 100 years), the flows generated with hyetographs were slightly lower than those obtained with maximum 24-hour rainfall (2.90 m³/s versus 5.71 m³/s, respectively).

Table 5. Physical-morphometric characteristics of the Yacupugro micro-basin.

A Km²	P Km	Lr Km	Max. El. m a.s.l.	Min. El. m a.s.l.	ΔH m	Ir m/m	Tc min.	Kc	Hm m a.s.l.
1.7	8.2	3.4	3960	2920	1040	0.31	15.2	1.7	3440

In terms of reliability, both methods are technically valid in the absence of observed data. However, in the present study, it was considered more prudent and reliable to use the highest flows obtained from 24-hour rainfall for hydraulic modeling, due to safety criteria. This approach ensures that the design of the urban drainage system is based on the worst-case scenario, which is advisable in rapid-response basins located in densely urbanized and highly vulnerable areas

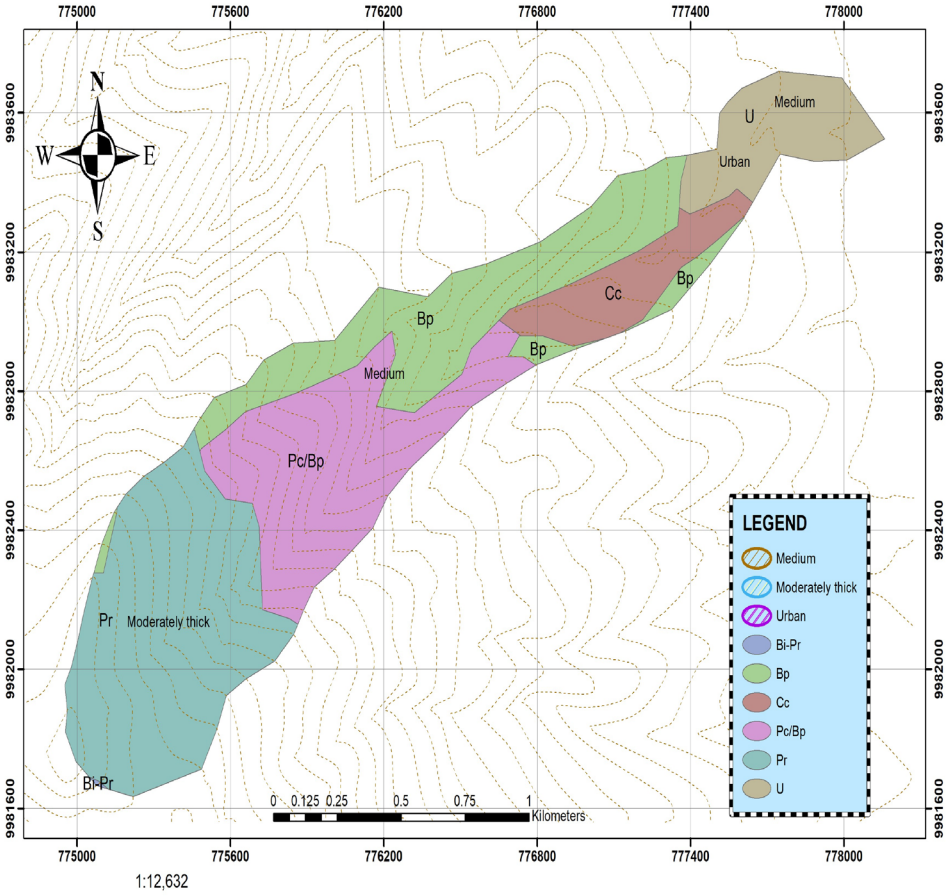

Figure. 3. Soil use and texture of the micro-basin of Q. Yacupugro.

.

3. RESULTS

The physical morphometric characteristics of the micro-basin were obtained with the help of ArcMap 10.5 software. With the information provided by the IGM, the land use map of the micro-basin was obtained, observing the following uses, being the upper part of the micro-basin is covered by moorland (Pr) in 33.24%, upper and central part covered by mixed crops (70% cultivated grass, 30% planted forest) (Pc/Bp) in 24.66%, planted forest (Bp) in 23.49%, short-cycle crops (Cc) in 8.34%, mixed crops (50% intervened forest, 50% moorland) (Bi-Pr) in a percentage of 0.04% and finally in the lower part the soil is urban (U) in a percentage of 10.24% (figure 3).

Where: A = area of the micro-basin (Km²), P= perimeter of the micro-basin (Km), Lr = length of the main channel (Km), Max. El. = maximum elevation (m a.s.l.), Min. El. = minimum elevation, (m a.s.l.), ΔH = level difference (m), Ir = slope of the main channel (m/m), Tc= time of concentration (minutes), Kc = Gravelius coefficient, Hm= average height (m a.s.l.) (Sassolas-Serrayet et al., 2018; Sandoval-Erazo &Toulkeridis, 2025).

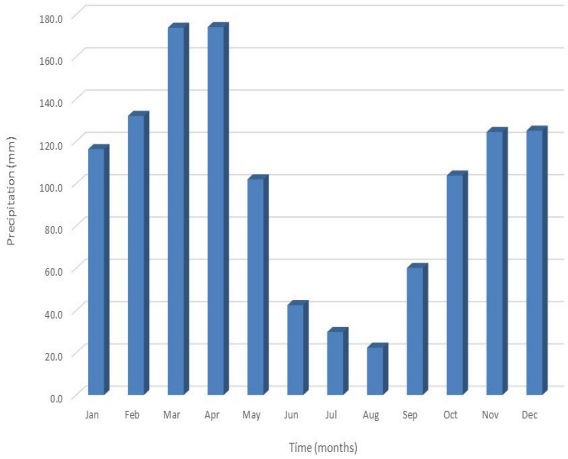

Figure. 4. Rainfall regime of the microbasin Yacupugro, at the station Antenas (P11), within the years of 2000-2022.

Table 6. Monthly rainfall values of the Yacupugro micro-basin (Station: Antennas, P11), 2000-2022.

Jan	Feb	Mar	Apr	May	Jun	Jul	Agu	Sep	Oct	Nov	Dec	Total
116.3	132	173.7	174	102	42.5	29.8	22.4	60.1	103.8	124.4	125	1206

With the given information of the types of texture and/or soils of the micro-basin, we observed that 59.60% of its surface corresponds to a medium texture, 33.81% to moderately coarse and 6.59% urban (figure 3). The rainfall in the micro-basin has a bimodal behavior with two well-differentiated rainy periods from January to May and from September to December, whose maximum peaks occur in the months of April (174.0 mm) and December (125.0 mm). The dry season goes from June to August with a minimum in the month of August (22.4 mm). The average annual rainfall is 1206.0 mm (figure 4 and table 6).

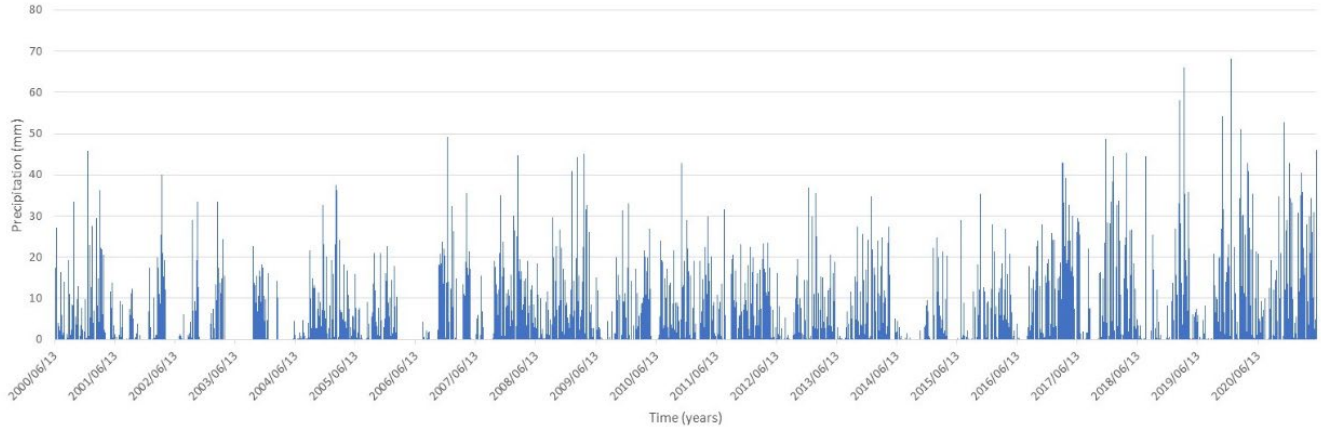

Figure. 5. Maximum daily rainfall, station Antenas (P11), for the years 2000-2022.

December is the month with the highest number of days with maximum daily precipitation, followed by February, March, November, January, April and January in order of frequency. The highest value in the series corresponds to the date of 12/31/2019 with a value of maximum daily precipitation of 68.2 mm, followed by a value of 52.7 mm corresponding to 11/20/2020 and a value of 49.2 mm dated 12/19/2006, while the other values in the series are in the range of 49.9 mm to 28.0 mm. With this analysis, it is clearer that the maximum daily precipitation occurs in the months of December (figure 5).

The 24-hour rainfall for different return periods at the Antenas station (P11) considering its best fit and considering that the rainfall in 24 hours is 1.13 times the daily rainfall, the following values are obtained (Fattahi & Habibi, 2022).

Table 7. 24-hour rainfall from Antenas P11 station.

Distribution laws	Return periods (Tr) - years			
	10	25	50	100
	Maximum rainfall in 24 hours - mm			
Gumbel (Tipo I)	63.0	72.3	73.9	85.3
Pearson III	60.3	68.1	73.8	79.4
Log Pearson III	59.7	67.6	73.5	79.8

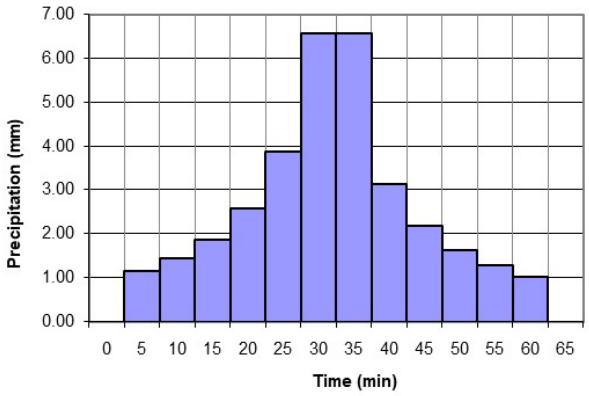

Figure. 6. Hyetograph with the return period of 10 years.

Using the La Chorrera station equation (2), the precipitation hyetographs of the micro-basin were obtained by applying the alternating block method (Pinheiro et al., 2024) for return periods (Tr) of 10, 25, 50 and 100 years, whose values are observed in Table 8 and figures 6, 7, 8 and 9.

Table 8. Hyetographs, microbasin Q. Yacupugro: Tr (10, 25, 50, 100 years), Tc= 0.253 h.

Precipitation hyetographs (mm)				
Duration (min)	Return period - years			
	10	25	50	100
0	0.00	0.00	0.00	0.00
5	1.14	1.26	1.35	1.46
10	1.43	1.58	1.70	1.83
15	1.87	2.07	2.22	2.39
20	2.58	2.85	3.07	3.30
25	3.87	4.28	4.60	4.95
30	6.56	7.25	7.80	8.39
35	6.56	7.25	7.80	8.39
40	3.12	3.45	3.71	3.99
45	2.18	2.41	2.59	2.79
50	1.63	1.80	1.94	2.08
55	1.27	1.41	1.51	1.63
60	1.03	1.13	1.22	1.31

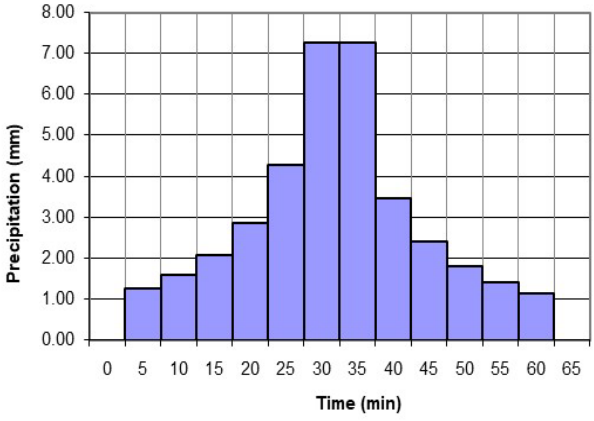

Figure. 7. Hyetograph, with the return period of 25 years.

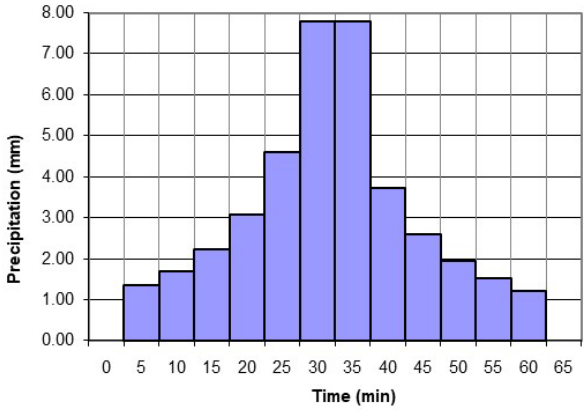

Figure. 8. Hyetograph, with the return period of50 years.

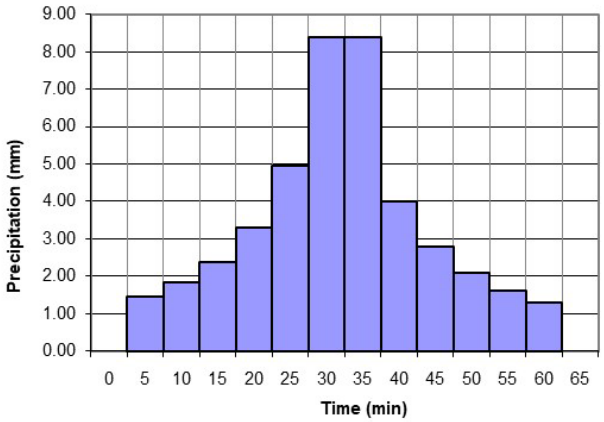

Figure. 9. Hyetograph, with the return period of 100 years.

3.1. Hydrological modelling

For the hydrological modeling of rainfall runoff, the average CNII values and physical parameters of the micro-basin were obtained, which are observed in tables 9 and 10.

Using data from tables 8 and 9, the micro-basin was modeled, obtaining hydrographs for 10, 25, 50 and 100 years of return period, with the hyetograph and the 100-year return period hydrograph being observed as a sample (figures 10 and 11)

Table 9. Curve number (CN II), Yacupugro micro-basin.

Land use	Area (km^2)	Percentage (%)	Soil texture	Area (km^2)	Percentage (%)	Hydrological classification	CNII
						D	66
50% intervened forest, 50% moorland	0.001	0.04%	Urbane	0.111	6.59%	------	------
			Moderately			A	55
Planted forest	0.361	21.45%	thick	0.569	33.81%		
Planted forest	0.034	2.04%	Media	1.002	59.60%	B	55
Short-cycle crop	0.140	8.34%	------	0.000	------	------	71
70% Cultivated pasture, 30% Planted forest	0.415	24.66%	------	0.000	------	------	79
Páramo	0.559	33.24%	------	0.000	------	------	39
Urban	0.172	10.24%	------	0.000	------	------	98
Total	1.682	100%	------	1.682	100%	Weighted CNII	61.34

Table 10. Data from the study micro-basin used in the HEC-HMS 4.11 rainfall-runoff model.

Micro-basin	Area (Km^2)	CN	Tc (min)	Tlag (min)	S (mm.)	% impermeable floor	Ia (mm)
Yacupugro	1.68	61.34	15.22	9.13	160.08	10	32.017

Using data from Tables 2 and 3, applying the SCS method for abstractions, flows were generated for return periods of 10, 25, 50 and 100 years, as indicated in the 50- and 100-year return period hydrograph (Figures 12 and 13).

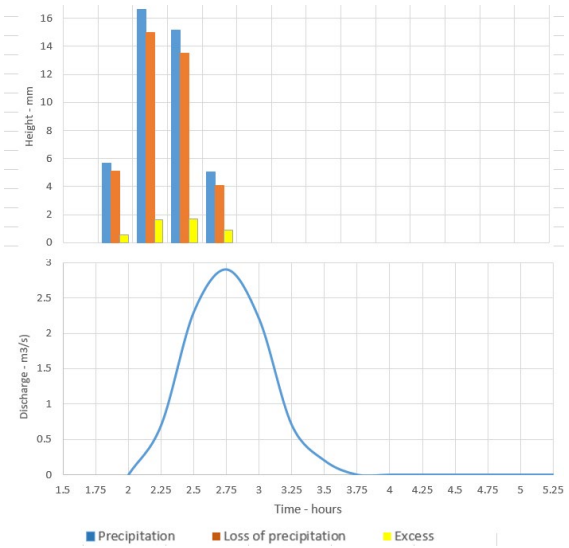

Figure. 10. Hyetograph and hydrograph-Tr100 years.

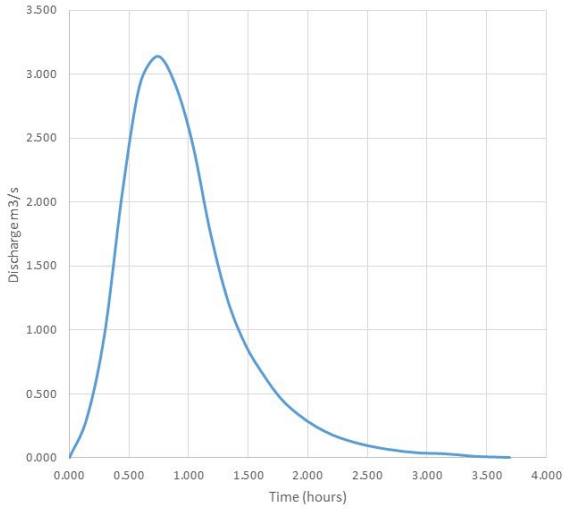

Figure. 11. Model hydrograph HECHMS4.11-Tr25 years.

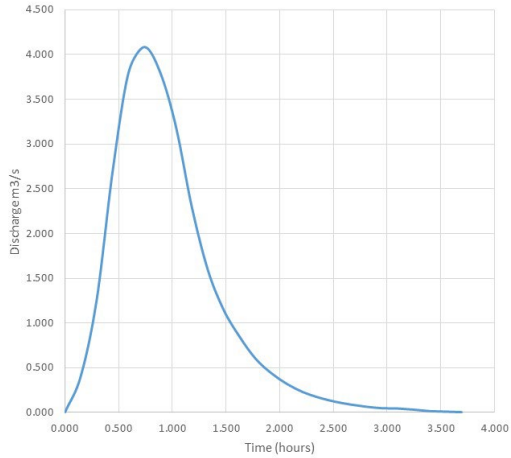

Figure. 12. SCS unit hydrograph – Tr50 years.

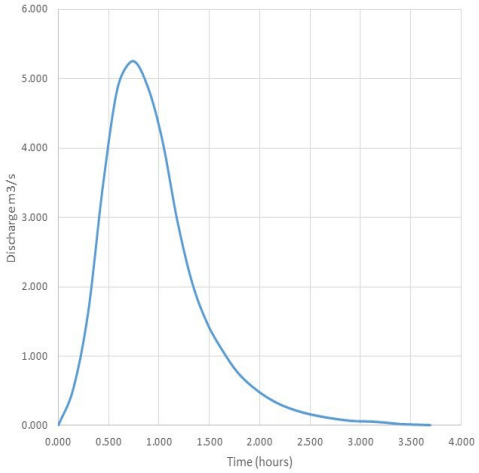

Figure. 13. SCS-Tr100-year unit hydrograph.

Finally, the flows obtained through hyetographs and maximum rainfall in 24 hours are listed in Table 11. The flows generated with the rainfall hyetographs are relatively slightly lower for high return periods in relation to those generated through maximum rainfall in 24 hours, but in general, since it is a flood estimate, it can be concluded that these values are acceptable and in the case of the present study, the highest values were taken for hydraulic modeling on the safety side.

Table 11. Maximum flows for return periods of 10, 25, 50 and 100 years – m^3/s, generated with hyetographs and with maximum rainfall in 24 hours of the Yacupugro micro-basin within an area of 1.68 Km^2.

Maximum flow rates – m^3/s			
Q_{TR} 10 years	**Q_{TR} 25 years**	**Q_{TR} 50 years**	**Q_{TR} 100 years**
Flow rates generated with hyetographs			
2.10	2.40	2.60	2.90
Flow rates generated with maximum rainfall in 24 hours			
2.244	3.508	4.571	5.71

The hyetograph method, as indicated in table 11, distributes rainfall over time, simulating how a storm event actually occurs. It considers initial losses, infiltration, and soil retention capacity, and therefore smooths peak flow. It therefore tends to be more conservative and realistic, especially for ordinary design events.

The 24-hour maximum rainfall method takes the total accumulated precipitation over 24 hours and assumes that all of this rainfall generates direct runoff. It is usually applied with a high runoff coefficient, especially in impervious or saturated areas. It does not consider the hourly distribution of rainfall, which overestimates peak flow. The use of the hyetograph method as a basis for design, validating it with the 24-hour method for extreme scenarios or sensitivity analyses. In floodability studies and hydraulic modeling, it is recommended to use the highest flow (5.71 m³/s) if an extreme or safety design scenario is desired.

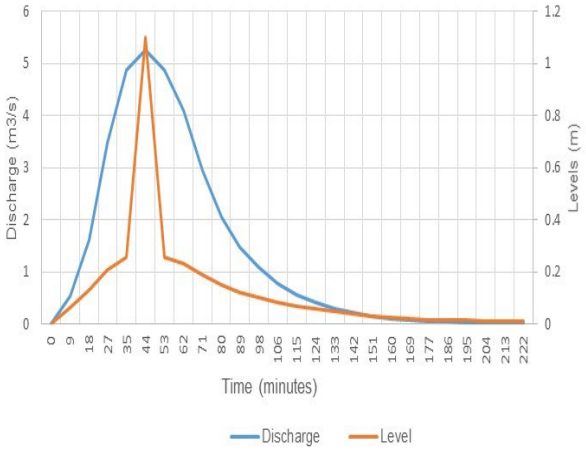

Figure. 14. Flow rate-level at channel junction.

3.3. Lamination growths

The reservoir achieves a decrease in peak flow from 7.60 m³/s to 2.60 m³/s and a delay of 45 minutes in the same reservoir with the Tr 100-year project storm and with the indicated conditions (Figure 9). Regarding storage, it is observed that up to 11,900 m³ is stored, reaching a height in the reservoir of 2.3 (graph 16) m, while continuing to drain a flow of 2.60 m³/s, without any overflow (Figure 17; Table 12).

The lamination results in a peak inlet flow rate of 7.60 m³/s, peak discharge of 2.6 m³/s, inlet volume of 11.06 mm, discharge volume of 11.71 mm, time to peak discharge of 3 hours and 15 minutes, peak storage of 11,900 m³ and maximum peak flood height of 202.7 m.

3.2. Rain-level-flow curves in the channel collecting waters

The simulated flows provide a rainfall-flow-level relationship at the junction of the Yacupugro micro-basin and the flow interception channel for a return period of 100 years, observing that the maximum level occurs when the flow is maximum, 45 minutes after the maximum rainfall pulse (figures 14 and 15). These figures also demonstrate the accumulated precipitation of the storm in red.

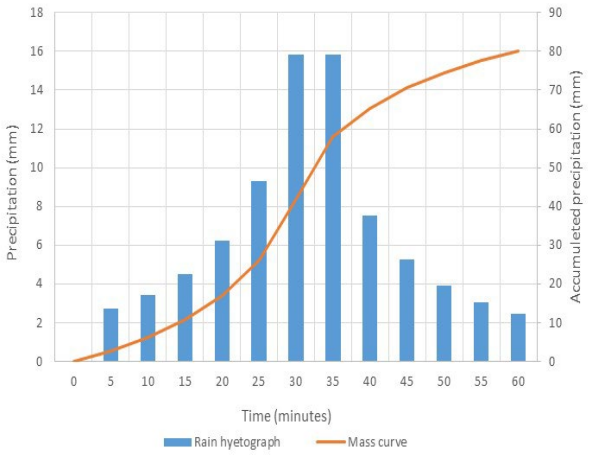

Figure. 15, Precipitation and accumulated rainfall.

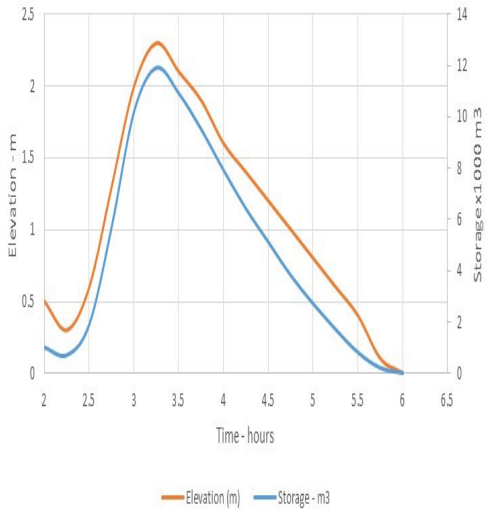

Figure. 16. Storage and Lift.

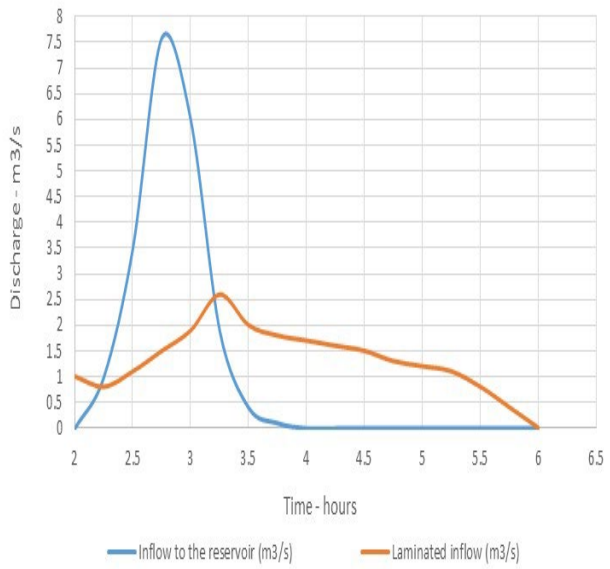

Figure. 17. Reservoir inflow hydrographs and flood lamination in reservoir (outflow).

Table 12. Reservoir modeling for flooding with a return period of 100 years.

Time	Q-income (m^3/s)	Reservoir ($1000m^3$)	Elevation (m)	Q-outflow (m^3/s)
02:00	0.0	1.0	200.5	1.0
02:15	1.0	07	200.3	0.8
02:30	3.5	1.9	200.6	1.1
02:45	7.6	5.7	201.3	1.5
03:00	6.0	10.2	202.0	1.9
03:15	1.9	11.9	202.3	2.6
03:30	0.4	10.9	202.1	2.0
03:45	0.1	9.5	201.9	1.8
04:00	0.0	7.9	201.6	1.7
04:15	0.0	6.4	201.4	1.6
04:30	0.0	5.1	201.2	1.5
04:45	0.0	3.8	201.0	1.3
05.00	0.0	2.7	200.8	1.2
05:15	0.0	1.7	200.6	1.1
05:30	0.0	0.8	200.4	0.8
05:45	0.0	0.2	200.1	0.4
06:00	0.0	0.0	200.0	0.0

3.4. Flood forecasting based on precipitation

It is estimated that this type of soil in the micro-basin would need to absorb at least 129 mm of water on average to reach field capacity, considering a depth of one meter. Normally, soils reach field capacity in the first month of the rainy season (between March-April and November-December), and during the remaining months, humidity remains close to or greater than field capacity; therefore, during the months of greatest rainfall, which are from January to May and from October to December, the soils are completely saturated, favoring the formation of floods. Based on the above, it can be said that the system can start with a warning if the rainfall in 3 to 7 days exceeds 129 mm. Subsequently, the rainfall must be monitored, separated by other events for a time of no more than 15 minutes (0.25 hours), as well as the levels of the micro-basin, generating alert levels as seen in Table 13.

Table 13. Rainfall thresholds for alert in the communities settled in the lower part of the Yacupugro micro-basin.

Alert type	Accumulated rainfall (mm)	Flow rate (m^3/s)	Micro-basin level (m a.s.l.)	Speed (m/s)	Approximate time for flooding
Green	20.0	9.46	3077.37 (level 0.00)	2.87	-------
Yellow	70.0	33.09	3078.45 (level 1.08 m)	4.35	-------
Red	115	54.37	3079.33 (level 1.96 m)	4.75	15 minutes

Regarding the accumulated rainfall of 129 mm during a period of 3 to 7 days, it has greater priority in the months of January, February, March, April, May, October, November, when the soils are at a humidity close to the field capacity (Shah & Suryanarayana, 2014). It is totally different if this precipitation event occurs at the beginning of the rainy season (January or September), when the soils are at a humidity close to the permanent wilting point, where they have their greatest infiltration potential and therefore their lowest runoff potential.

4. DISCUSSION

Some of the authors mentioned in this bibliography have used a variety of methods to estimate rainfall-runoff and flooding processes, based on hydrometeorological data, soil moisture, among others. In this regard, we have a software which analyzes the development of empirical models that predict the sensitivity of runoff to variations in precipitation, which can improve the predictability of floods in small basins by using the basin moisture

index, thus improving the understanding of hydrological variability and the response to climate change (Viana et al., 2022).

One of the criteria applied in this research is modeling for a maximum rainfall of 100-year return period by applying IDF curves, which allowed defining the thresholds of accumulated precipitation and flood levels, a similar criterion, where the interpretation of historical events and comparison of intensity-duration-frequency curves with those determined in other countries estimates that possible trigger thresholds for these events are in the range of rainfall with 50-100 years of return, with only 30-40 mm of precipitation in 30-60 minutes and (Li et al., 2021) also used meteorological models of frequency storms and the SCS in order to model floods of a certain probability from distributed rainfall of 24 h, in the absence of pluviographic observation to estimate flood flows for defined return periods such as 100 years. Investigations such as Probabilistic Urban Flash Flood Information Nexis (PUFFIN) are used to forecast flash floods up to three days before a storm approaches using a combination of deterministic and probabilistic precipitation forecasts similar to the soil moisture and antecedent precipitation-based model used to forecast flash flooding three days in advance in micro-basins (Shah & Suryanarayana, 2014).

Other existing models (Babu & Kumar, 2024), perform flow forecasting by combining the HEC-HMS model with a genetic algorithm neural network (GANN) and an ANFIS, obtaining results in which the HEC-HMS could not predict the flow discharge individually, so since it is a small micro-basin, it is proposed to forecast floods based on soil moisture (Shah & Suryanarayana, 2014).

The flood forecast in the Yacupugro micro-basin of the Metropolitan District of Quito, Ecuador, considers the integration of quantitative precipitation forecasts with real-time hydrology and hydraulic modeling towards the probabilistic forecast of urban floods used in (Moore, 1999; Nguyen et al., 2020; Werner et al., 2005).

The analysis of the methodology applied in the present research takes the concept that as the rain event(s) develop, the soil becomes saturated, the floods begin and move, it is necessary to monitor the levels reached and compare them with the alert levels for both rainfall and calculated levels, which will help to better assess a flood prediction, allowing the alert thresholds to be further calibrated (Tellman et al., 2018; Stevaux et al., 2009; Hardoy et al., 2011).

The alternate block method allowed the generation of design storms through the IDF curves at the Yacupugro micro-basin site, where in studies it is mentioned that the alternate block method is in fact a conservative approach to model design storms, especially when the historical data of the hyetograph are insufficient (Alamoudi et al., 2023; Viana et al., 2022).

The data of average daily rainfall increased by 13% (Fattahi & Habibi, 2022) were used for the generation of flows through the concept of unitary hydrograph, a similar concept is used, which mentions that in the absence of representative observed hyetographs, they can be reconstructed from the average daily rainfall by microbasins or submicrobasins and must be displaced with respect to the peak of the hydrograph in a time equal to the Tdp of the same, if this is unknown, the Tc calculated from the center of gravity can be used (Silva et al., 2022).

Although the warning network measurements are accurate and reliable, it is observed that the forecasts may differ from the observed ones and it is necessary to have real-time measurements to corroborate and adjust the forecast, so the forecast thresholds must be calibrated over time as the rain and flash flood events occur in the Yacupugro micro-basin (Pawar & Patil, 2022).

Predicting the areas prone to flash floods is essential for proactive disaster management. However, it is difficult to obtain such predictions accurately with physical hydrological models due to the scarcity of flood observation stations and the lack of monitoring systems (Guelfi & López-Vazquez, 2018; Shih & Hamrick, 1975), so in the current research the flood forecast is made based on the precipitation and the antecedent soil moisture close to the field capacity, whose parameters must be calibrated over time until obtaining reliable precipitation thresholds and levels for forecasting (Sharif & Miller, 2006).

The results obtained demonstrate that the Yacupugro microbasin exhibits typical rapid-response basin behavior, with very short times of concentration and high peak flows for moderate rainfall events. However, notable differences are

evident between the flows estimated using synthetic hyetographs and those derived from 24-hour maximum rainfall, especially for long return periods (e.g., 2.90 vs. 5.71 m³/s for Tr = 100 years). These discrepancies are due to the different temporal concentrations of each method, with the latter being more conservative. This highlights the importance of appropriately selecting design events.

A major limitation of the study is the lack of flow records, which prevents model calibration and validation. Although standard methods (CN, SCS hydrograph) were used, their performance depends on local land-use conditions and antecedent moisture, which can vary spatially and temporally.
The lack of rainfall data also forced the use of synthetic hyetographs based on IDF curves, which, while useful, may not adequately reflect local convective rainfall. The future installation of an automatic rainfall and streamflow stations is recommended to improve system reliability.

From an operational perspective, the proposed system, based on accumulated precipitation thresholds, has already been tested in similar studies and allows for early warnings even without real-time sensors. However, the 129 mm threshold should be interpreted with caution and adjusted based on new information. Comparing it with thresholds in similar watersheds in the Andean region would strengthen its validity and applicability. Summarizing, the model is a useful, low-cost tool, especially valuable for expanding urban areas with high-risk exposure and limited hydrometeorological instrumentation.

The methods and results presented in this research improve the understanding of the degree to which incremental changes in land use can significantly alter the reality of flood risk in micro-watersheds undergoing urbanization (Cheng et al., 2021), such as the Yacupugro micro-watershed, which is undergoing urbanization due to invasions that occur continuously on the slopes of Pichincha in the Metropolitan District of Quito, Ecuador.

5. CONCLUSIONS

This study developed a rapid-response flood forecasting methodology for urban microwatersheds, applying it to the Yacupugro microwatershed in Quito, Ecuador. The HEC-HMS 4.11 hydrological model was used, along with hyetographs generated from IDF curves and 24-hour maximum rainfall, using the Curve Number (CN) method and the SCS unit hydrograph as the basis for runoff estimation.

From a quantitative perspective, peak flows obtained for a 100-year return period were 2.90 m³/s using IDF hyetographs and 5.71 m³/s with 24-hour maximum rainfall. The latter approach, however, was found to produce more conservative results. Therefore, the latter approach was chosen for the hydraulic design, prioritizing safety. Likewise, it was determined that a previous rainfall of 129 mm accumulated over 3 to 7 days represents a critical threshold for triggering early warnings, given its relationship with soil saturation.

However, the study has significant limitations. The main one is the lack of gauged streamflow data, which prevented direct calibration and validation of the model. Furthermore, the lack of pluviographic records limited the temporal accuracy of the rainfall events used. Consequently, the results should be considered preliminary estimates subject to verification and adjustment.

Based on the findings, at least four main lines of future research are proposed, being (1) to improve data acquisition by installing automatic rainfall and level stations in the watershed; (2) to couple the hydrological model with real-time data sources, such as weather radars or satellite images, to allow forecast updates under dynamic conditions; (3) to compare the proposed alert threshold with similar studies in other Andean urban micro-watersheds to assess its validity and regional transferability; and also (4) to explore indirect calibration techniques using historical emergency event data or community reports.

Overall, the applied methodology constitutes an operational, flexible, and low-cost tool, particularly useful for developing urban contexts where resources for hydrological monitoring are limited.

6. REFERENCES

Abraham, S., Huynh, C., & Vu, H. (2019). Classification of soils into hydrologic groups using machine learning. *Data*, *5*(1), 2.

Al-Dughairi, A. A. (2023). Runoff hydrographs using Snyder and SCS synthetic unit hydrograph methods: A case study of ungauged watersheds of

Imam Turki Bin Abdullah Royal Nature Reserve (ITBA)-Saudi Arabia. □□□□□□ □□□□ □□□□□□□□ □ □□□□□□□□ 94-79), 3(7 ,□□□□□□□□□□□.

Alamoudi, F., Saber, M., Kantoush, S. A., Boulmaiz, T., Abdrabo, K. I., Abdelmoneim, H., & Sumi, T. (2023). Stormwater management modeling and machine learning for flash flood susceptibility prediction in Wadi Qows, Saudi Arabia. *Hydrological Research Letters*, *17*(3), 62-68.

Albán-Campaña, D. D., Zapata, J., Ordoñez, E., Toulkeridis, T., Rodriguez, K., Martinez-Maldonado, K. P., & Zapata, A. (2021, June). Evaluation of Subsidence Hazard with Geo-Radar Within a Populated City-A Case Study of Southern Quito, Ecuador. In *XV Multidisciplinary International Congress on Science and Technology* (pp. 169-183). Cham: Springer International Publishing.

Alonso-Pandavenes, O., Torrijo Echarri, F. J., & Garzón-Roca, J. (2024). Sustainable Management of Landslides in Ecuador: Leveraging Geophysical Surveys for Effective Risk Reduction. *Sustainability*, *16*(24), 10797.

Assi, A. T., Blake, J., Mohtar, R. H., & Braudeau, E. (2019). Soil aggregates structure-based approach for quantifying the field capacity, permanent wilting point and available water capacity. *Irrigation Science*, *37*, 511-522.

Babu, S. H., & Kumar, D. S. (2024, June). Application of the HEC-HMS model to generate a flood hydrograph of an extreme event in a tropical basin. In *IOP Conference Series: Earth and Environmental Science* (Vol. 1326, No. 1, p. 012145). IOP Publishing

Bajirao, T. S. (2021). Comparative performance of different probability distribution functions for maximum rainfall estimation at different time scales. *Arabian Journal of Geosciences*, *14*, 1-15.

Bell, F. C., & Kar, S. O. (1969). Characteristic response times in design flood estimation. *Journal of Hydrology*, *8*(2), 173-196.

Bendix, J., Trachte, K., Palacios, E., Rollenbeck, R., Göttlicher, D., Nauss, T., & Bendix, A. (2011). El Niño meets la Niña—anomalous rainfall patterns in the" traditional" el Niño region of Southern Ecuador. *Erdkunde*, 151-167.

Brachhi, P., Torrijo, F. J., Boix, A., Cruz Cabrera, M., & Giordanelli, D. (2020). Urban and hydrogeological alert on the morphoclimatic risk affecting Quito's World Heritage. *International Archives of the Photogrammetry, Remote Sensing and Spatial Information Sciences (Online)*, *44*, 825-832.

Brendel, C. E., Dymond, R. L., & Aguilar, M. F. (2020). Integration of quantitative precipitation forecasts with real-time hydrology and hydraulics modeling towards probabilistic forecasting of urban flooding. *Environmental Modelling & Software*, *134*, 104864.

Bucherie, A., Hultquist, C., Adamo, S., Neely, C., Ayala, F., Bazo, J., & Kruczkiewicz, A. (2022). A comparison of social vulnerability indices specific to flooding in Ecuador: Principal component analysis (PCA) and expert knowledge. *International journal of disaster risk reduction*, *73*, 102897.

Cann, K. F., Thomas, D. R., Salmon, R. L., Wyn-Jones, A. P., & Kay, D. (2013). Extreme water-related weather events and waterborne disease. *Epidemiology & Infection*, *141*(4), 671-686.

Castelo, C. A. J., Cruz, M., Almeida, O. P., & Toulkeridis, T. (2018, April). Comparative determination of the probability of landslide ocurrences and susceptibility in Central Quito, Ecuador. In *2018 International Conference on eDemocracy & eGovernment (ICEDEG)* (pp. 136-143). IEEE.

Cheng, D., Shimizu, K., & Yamada, T. J. (2021). Hydrological frequency analysis of large-ensemble climate simulation data using control density as a statistical control. *Hydrological Research Letters*, *15*(4), 84-91.

Chow, V. T. (1953). Frequency analysis of hydrologic data with special application to rainfall intensities. *University of Illinois. Engineering Experiment Station. Bulletin; no. 414*.

Daly, M. C. (1989). Correlations between Nazca/Farallon plate kinematics and forearc basin evolution in Ecuador. *Tectonics*, *8*(4), 769-790.

De Moraes, O. L. L. (2022). Some evidence on the reduction of the disasters impact due to natural hazards in the Americas and the Caribbean after the 1990s. *International Journal of Disaster Risk Reduction*, *75*, 102984.

Dibaba, W. T. (2018). A review of sustainability of urban drainage system: traits and consequences. *Journal of Sedimentary Environments*, *3*(3), 131-137.

Domínguez-Castro, F., García-Herrera, R., & Vicente-Serrano, S. M. (2018). Wet and dry extremes in Quito (Ecuador) since the 17th century. *International Journal of Climatology*, *38*(4), 2006-2014.

EMAAP-Q (Alcantarillado, Empresa Metropolitana de, and Agua Potable) 2009. 'Normas de Diseño de Sistemas de Alcantarillado Para La EMAAP-Q'. *Quito, Ecuador*.

Fattahi, E., & Habibi, M. (2022). Estimation of probable maximum precipitation 24-h (PMP 24-h) through statistical methods over Iran. *Water Supply*, *22*(8), 6543-6557.

Gopalakrishnan, C. (2013). Water and disasters: A review and analysis of policy aspects. *International Journal of Water Resources Development*, *29*(2), 250-271.

Grayman, W. M. (2011). Water-related disasters: A review and commentary. *Frontiers of Earth Science*, *5*(4), 371-377.

Guelfi, M., & López-Vazquez, C. (2018). Comparing the Thiessen's Method against simpler alternatives using Monte Carlo Simulation. *Revista Cartográfica*, (96), 125-138.

Guo, J. (2022). General unit hydrograph from Chow's linear theory of hydrologic systems and its applications. *Journal of Hydrologic Engineering*, *27*(10), 04022020.

Hamidifar, H., & Nones, M. (2021). Global to regional overview of floods fatality: the 1951–2020 period. *Natural Hazards and Earth System Sciences Discussions*, *2021*, 1-22.

Hardoy, J., Pandiella, G., & Barrero, L. S. V. (2011). Local disaster risk reduction in Latin American urban areas. *Environment and Urbanization*, *23*(2), 401-413.

Hederra, R. (1987). Environmental sanitation and water supply during floods in Ecuador(1982-1983). *Disasters*, *11*(4), 297-309.

Jaillard, E., Hérail, G., Monfret, T., Díaz-Martínez, E., Baby, P., Lavenu, A., ... & Campos, D. (2000). Tectonic evolution of the Andes of Ecuador, Peru, Bolivia and northern Chile. *Tectonic evolution of South America, edited by: Cordani, UG, Milani, E. J., Thomaz Filho, A., and Campos, DA, Rio de Janeiro, Brazil*, 481-559.

Jankowfsky, S., Sharifian, M., Moges, E., Nicotina, L., Li, S., & Hilberts, A. (2024). *How appropriate is the alternating block method to represent flooding from extreme precipitation events?* (No. EGU24-6064). Copernicus Meetings.

Jonkman, S. N. (2005). Global perspectives on loss of human life caused by floods. *Natural hazards*, *34*(2), 151-175.

Jonkman, S. N., & Kelman, I. (2005). An analysis of the causes and circumstances of flood disaster deaths. *Disasters*, *29*(1), 75-97.

Koop, S. H., & van Leeuwen, C. J. (2017). The challenges of water, waste and climate change in cities. *Environment, development and sustainability*, *19*(2), 385-418.

Lee, J., Perera, D., Glickman, T., & Taing, L. (2020). Water-related disasters and their health impacts: A global review. *Progress in Disaster Science*, *8*, 100123.

Li, X., Erpicum, S., Mignot, E., Archambeau, P., Pirotton, M., & Dewals, B. (2021). Influence of urban forms on long-duration urban flooding: Laboratory experiments and computational analysis. *Journal of Hydrology*, *603*, 127034.

Liu, Q., Yuan, J., Yan, W., Liang, W., Liu, M., & Liu, J. (2023). Association of natural flood disasters with infectious diseases in 168 countries and territories from 1990 to 2019: a worldwide observational study. *Global Transitions*, *5*, 149-159.

Liu, T., Shi, P., & Fang, J. (2022). Spatiotemporal variation in global floods with different affected areas and the contribution of influencing factors to flood-induced mortality (1985–2019). *Natural Hazards*, *111*(3), 2601-2625.

Lonsdale, P. (1978). Ecuadorian subduction system. *AAPG Bulletin*, *62*(12), 2454-2477.

Loor, I. (2024). Unveiling the dynamics of informal settlements in quito: occupation, organisation, and infrastructure challenges. *GeoJournal*, *89*(2), 76.

Macías, L., Quiñonez-Macías, M., Toulkeridis, T., & Pastor, J. L. (2024). Characterization and geophysical evaluation of the recent 2023 Alausí landslide in the northern Andes of Ecuador. *Landslides*, *21*(3), 529-540.

Macías, L., Bonifaz, H., Toulkeridis, T., & Pastor, J. L. (2025). Geotechnical and geophysical evaluation of the remarkable Chunchi landslide of 2021 in the Andean Ecuador. *Natural Hazards*, 1-23.

Marengo, J. A., Cardona, O. D., & Martinez, R. (2022). Climatic hazards and disaster risk reduction in South-Central America and the Caribbean. *Frontiers in Climate*, *4*, 1111676.

Marrero, J. M., Yepes, H., Salazar, P., & Lara, S. (2023). Urbicide or Suicide? Shaping Environmental Risk in an Urban Growth Context: The Example of Quito City (Ecuador). In *Urbicide: The Death of the City* (pp. 263-291). Cham: Springer International Publishing.

Mato, F., & Toulkeridis, T. (2017). THE MISSING LINK IN EL NIÑO'S PHENOMENON GENERATION. *Science of tsunami hazards*, *36*(3).

McDonald, R. I., Kareiva, P., & Forman, R. T. (2008). The implications of current and future urbanization for global protected areas and biodiversity conservation. *Biological conservation*, *141*(6), 1695-1703.

Mejia, S. N., Paz, S. M., Tabari, H., Singaña-Chasi, M., Paredes, D., & Willems, P. (2023). *Climate change impacts on IDF curves, urban flooding, and river discharge in Quito, Ecuador* (No. EGU23-17185). Copernicus Meetings.

Mendoza, B., Fiallos, M., Iturralde, S., Santillán, P., Guananga, N., Bejar, J., ... & Sándor, Z. (2021). Determination of field capacity in the Chibunga and Guano rivers micro-basins. *F1000Research*, *10*.

Mokuolu, O. A., Odunaike, A. K., Iji, J. O., & Aremu, A. S. (2022). Assessing the effects of solid wastes on urban flooding: A case study of Isale Koko. *LAUTECH Journal of Civil and Environmental Studies*, *9*(1), 22-30.

Moncayo-Galárraga, D. S., Robayo-Nieto, A. A., Padilla, O., & Toulkeridis, T. (2022, November). Implementation of the CAESAR-Lisflood cellular automated landscape evolution model to determine possible flood areas in the Portoviejo river sub-basin, Coastal Ecuador. In *International Conference on Applied Technologies* (pp. 212-227). Cham: Springer Nature Switzerland.

Moore, M., Gould, P., & Keary, B. S. (2003). Global urbanization and impact on health. *International journal of hygiene and environmental health*, *206*(4-5), 269-278.

Moore, R. J. (1999). Real-time flood forecasting systems: Perspectives and prospects. *Floods and landslides: Integrated risk assessment*, 147-189.

Nguyen, H. T., Duong, T. Q., Nguyen, L. D., Vo, T. Q., Tran, N. T., Dang, P. D., ... & Nguyen, L. K. (2020). Development of a spatial decision support system for real-time flood early warning in the Vu Gia-Thu Bon river basin, Quang Nam Province, Vietnam. *sensors*, *20*(6), 1667.

Oliveira, E. C. L. D., Nogueira Neto, A. V., Santos, A. P. P. D., da Costa, C. P. W., Freitas, J. C. G. D., Souza-Filho, P. W. M., ... & Tedeschi, R. G. (2023). Precipitation forecasting: from geophysical aspects to machine learning applications. *Frontiers in Climate*, *5*, 1250201.

Orejuela, I. P., & Toulkeridis, T. (2020, April). Evaluation of the susceptibility to landslides through diffuse logic and analytical hierarchy process (AHP) between Macas and Riobamba in Central Ecuador. In *2020 Seventh international conference on eDemocracy & eGovernment (ICEDEG)* (pp. 201-207). IEEE.

Pabón-Caicedo, J. D., Arias, P. A., Carril, A. F., Espinoza, J. C., Borrel, L. F., Goubanova, K., ... & Villalba, R. (2020). Observed and projected hydroclimate changes in the Andes. *Frontiers in Earth Science*, *8*, 61.

Pawar, B., & Patil, K. A. (2022). Analysis of Morphometric Parameters of Watershed Using GIS. In *Recent Trends in Construction Technology and Management: Select Proceedings of ACTM*

2021 (pp. 603-612). Singapore: Springer Nature Singapore.

Peltre, P. (1989). Quebradas y riesgos naturales en Quito, período 1900-1988. *Estudios de geografía*, *2*, 45-65.

Pillosu, F. M., Bucherie, A., Kruczkiewicz, A., Haiden, T., Baugh, C., Hultquist, C., ... & Cloke, H. L. (2024). Can global rainfall forecasts identify areas at flash flood risk? Proof of concept for Ecuador. *ECMWF Technical Memo*, (917).

Pinheiro, S. A. R., Reis, G. B., de Souza Fraga, M., da Silva, D. D., Abreu, M. C., & Parma, L. M. (2024). Flow regionalization using precipitation data from different bases as a predictive variable. *Physics and Chemistry of the Earth, Parts A/B/C*, *133*, 103516.

Pinos, J., & Quesada-Román, A. (2021). Flood risk-related research trends in Latin America and the Caribbean. *Water*, *14*(1), 10.

Pinos, J., & Timbe, L. (2020). Mountain riverine floods in Ecuador: Issues, challenges, and opportunities. *Frontiers in Water*, *2*, 545880.

Poma, J., Gualotuña, D., & Álvarez, C. (2024, September). Mass Movement Risk Assessment with Drone and GPS Technology: A Case Study in Quito, Ecuador. In *2024 IEEE ANDESCON* (pp. 1-6). IEEE.

Poma, P., Polanco, M., Usca, K., Casella, C., & Toulkeridis, T. (2025). An Evaluation of the Public Service of the Integrated Municipal Management of Urban Solid Waste in the Galapagos and the Amazonian Region of Ecuador. *Sustainability*, *17*(3), 1066.

Poma, P., Usca, M., & Toulkeridis, T. (2022, November). Evaluation of the Environmental Impacts Generated by the Management of Urban Solid Waste in the Open Waste Dump in Loreto, Eastern Ecuador. In *International Conference on Applied Technologies* (pp. 466-481). Cham: Springer Nature Switzerland.

Poma, P., Usca, M., Fdz-Polanco, M., Garcia-Villacres, A., & Toulkeridis, T. (2021). Landslide and environmental risk from oil spill due to the rupture of SOTE and OCP pipelines, San Rafael Falls, Amazon Basin, Ecuador. *Int. J. Adv. Sci. Eng. Inf. Technol*, *11*(4), 1558-1566.

Poveda, G., Espinoza, J. C., Zuluaga, M. D., Solman, S. A., Garreaud, R., & Van Oevelen, P. J. (2020). High impact weather events in the Andes. *Frontiers in Earth Science*, *8*, 162.

Puente-Sotomayor, F., Egas, A., & Teller, J. (2021). Land policies for landslide risk reduction in Andean cities. *Habitat international*, *107*, 102298.

Raleigh, C. (2011). The search for safety: The effects of conflict, poverty and ecological influences on migration in the developing world. *Global Environmental Change*, *21*, S82-S93.

Reyes Pozo, M. D., Moreno Izquierdo, V. J., López Alulema, A. C., Lasso Benítez, L. D. P., Suango Sanchez, V. D. R., & Toulkeridis, T. (2020, November). Use of the heuristic model and GIS to zone landslide hazards in the Mira River Basin, Ecuador. In *Conference on Information and Communication Technologies of Ecuador* (pp. 243-257). Cham: Springer International Publishing.

Rojas, T., Dunning, P., & Sisa, I. (2022). Lifeguard Training Program and Drowning Death Rates in Ecuador, 2000–2019. *American journal of public health*, *112*(11), 1546-1550.

Rosales-Rueda, M. (2018). The impact of early life shocks on human capital formation: Evidence from El Niño floods in Ecuador. *Journal of health economics*, *62*, 13-44.

Sahu, M. K., Shwetha, H. R., & Dwarakish, G. S. (2024). Unravelling flood complexity: statistical and neural network approaches for Cauvery River Basin, India. *Natural Hazards*, *120*(15), 14495-14528.

Salami, A. W., Bilewu, S. O., Ibitoye, B. A., & Ayanshola, M. A. (2017). Runoff hydrographs using Snyder and SCS synthetic unit hydrograph methods: A case study of selected rivers in south west Nigeria. *Journal of Ecological Engineering*, *18*(1).

Salcedo, D., Padilla Almeida, O., Morales, B., & Toulkeridis, T. (2022, January). Smart city planning based on landslide susceptibility mapping using fuzzy logic and multi-criteria evaluation techniques in the city of quito, ecuador. In *Doctoral Symposium on Information and Communication Technologies-*

DSICT (pp. 89-103). Cham: Springer International Publishing.

Salcedo, D., Padilla Almeida, O., Morales, B., & Toulkeridis, T. (2018). Landslide susceptibility mapping using fuzzy logic and multi-criteria evaluation techniques in the city of Quito, Ecuador. *Natural Hazards and Earth System Sciences Discussions*, *2018*, 1-33.

Sandoval Erazo, W., Toulkeridis, T., Aguilar Ponce, A., Chiriboga, S. E., & Salazar, E. (2021, June). Risk and vulnerability analysis of flood hazards in the Colón Parrish, western Ecuador based on HEC-RAS numerical simulation. In *XV Multidisciplinary International Congress on Science and Technology* (pp. 245-260). Cham: Springer International Publishing.

Sandoval-Erazo, W. and Toulkeridis, T., 2025: Concentration Time Analysis – Case study of the Mal Paso River Basin, Ecuador. Submitted

Santos, T., Martins, C. C., Schneider, G., Hochwart, B., & Triani, B. (2023). On the intersection of international security, defense, and climate change in Latin America and the Caribbean. *Brazilian Journal of International Relations*, *11*(2), 282-308.

Sarker, B., Keya, K. N., Mahir, F. I., Nahiun, K. M., Shahida, S., & Khan, R. A. (2021). Surface and ground water pollution: causes and effects of urbanization and industrialization in South Asia. *Scientific Review*, *7*(3), 32-41.

Sarmiento, F. O. (2009). Geomorphology of natural hazards and human-induced disasters in Ecuador. *Developments in Earth Surface Processes*, *13*, 149-163.

Sassolas-Serrayet, T., Cattin, R., & Ferry, M. (2018). The shape of watersheds. *Nature communications*, *9*(1), 3791.

Schreider, S. Y., Smith, D. I., & Jakeman, A. J. (2000). Climate change impacts on urban flooding. *Climatic Change*, *47*, 91-115.

Sekovski, I., Newton, A., & Dennison, W. C. (2012). Megacities in the coastal zone: Using a driver-pressure-state-impact-response framework to address complex environmental problems. *Estuarine, Coastal and Shelf Science*, *96*, 48-59.

Shah, K., & Suryanarayana, T. M. V. (2014). Characterization and Frequency Analysis of One Day Annual Maximum and Two to Seven Consecutive Days' Maximum Rainfall of Panam Dam, Gujarat, India. *International Journal of Engineering Trends and Technology (IJETT)*, *13*(2), 76-80.

Sharif, H., & Miller, N. L. (2006, January). Hydroclimatological predictions based on basin's humidity index. In *Conf. on Climate Variability and Change, 18th, Atlanta, GA* (Vol. 28).

Shih, S. F., & Hamrick, R. L. (1975). A modified Monte Carlo technique to compute Thiessen coefficients. *Journal of Hydrology*, *27*(3-4), 339-356.

Silva, J. R. I., de Assunção Montenegro, A. A., de Andrade Farias, C. W. L., Jardim, A. M. D. R. F., da Silva, T. G. F., & Montenegro, S. M. G. L. (2022). Morphometric characterization and land use of the Pajeú river basin in the Brazilian semi-arid region. *Journal of South American Earth Sciences*, *118*, 103939.

Singh, R. L., & Singh, P. K. (2017). Global environmental problems. *Principles and applications of environmental biotechnology for a sustainable future*, 13-41.

Sivakumar, B. (2011). Global climate change and its impacts on water resources planning and management: assessment and challenges. *Stochastic Environmental Research and Risk Assessment*, *25*, 583-600.

Stevaux, J. C., Latrubesse, E. M., Hermann, M. L. D. P., & Aquino, S. (2009). Floods in urban areas of Brazil. *Developments in Earth Surface Processes*, *13*, 245-266.

Tellman, B., McDonald, R. I., Goldstein, J. H., Vogl, A. L., Flörke, M., Shemie, D., ... & Veiga, F. (2018). Opportunities for natural infrastructure to improve urban water security in Latin America. *PLoS One*, *13*(12), e0209470.

Toapanta, R., Chafla, J., & Toapanta, A. (2020, October). Physical variables monitoring to contribute to landslide mitigation with IoT-based systems. In *The International Conference on Advances in Emerging Trends and*

Technologies (pp. 58-71). Cham: Springer International Publishing.

Toulkeridis, T., & Zach, I. (2017). Wind directions of volcanic ash-charged clouds in Ecuador–implications for the public and flight safety. *Geomatics, Natural Hazards and Risk*, *8*(2), 242-256.

Toulkeridis, T., Rodríguez, F., Arias Jiménez, N., Baile, D. S., Martínez, R. S., Addison, A., ... & Díaz Perez, C. (2016). Causes and consequences of the sinkhole at El Trébol of Quito, Ecuador–implications for economic damage and risk assessment. *Natural Hazards and Earth System Sciences*, *16*(9), 2031-2041.

Toulkeridis, T., Simón Baile, D., Rodríguez, F., Salazar Martínez, R., Arias Jiménez, N., & Carreon Freyre, D. (2015). Subsidence at the "Trébol" of Quito, Ecuador: an indicator for future disasters?. *Proceedings of the International Association of Hydrological Sciences*, *372*(372), 151-155.

Toulkeridis, T., Tamayo, E., Simón-Baile, D., Merizalde-Mora, M. J., Reyes–Yunga, D. F., Viera-Torres, M., & Heredia, M. (2020). Cambio Climático según los académicos ecuatorianos-Percepciones versus hechos. *LA GRANJA. Revista de Ciencias de la Vida*, *31*(1), 21-46.

Trizio, F., Garzón-Roca, J., Eguibar, M. Á., Bracchi, P., & Torrijo, F. J. (2022). Above the Ravines: Flood Vulnerability Assessment of Earthen Architectural Heritage in Quito (Ecuador). *Applied Sciences*, *12*(23), 11932.

Troncoso, L., Torrijo, F. J., Ibadango, E., Pilatasig, L., Alonso-Pandavenes, O., Mateus, A., ... & Viteri, F. (2024). Analysis of the Impact Area of the 2022 El Tejado Ravine Mudflow (Quito, Ecuador) from the Sedimentological and the Published Multimedia Documents Approach. *GeoHazards*, *5*(3), 596-620.

Valdivieso-García, K., Vázquez-Patiño, A., Saritama, H., Contreras, J., Avilés, A., & García, F. (2024). Influence of climate change on precipitation extremes in Ecuador. *Climatic Change*, *177*(11), 165.

Vallejo, R. Z., Almeida, O. P., D'Howitt, M. C., Toulkeridis, T., Rodriguez, F., Mato, F., & Muñoz, B. M. (2018, April). Numerical probability modeling of past, present and future landslide occurrences in Nothern Quito, Ecuador. In *2018 International Conference on eDemocracy & eGovernment (ICEDEG)* (pp. 117-125). IEEE.

Veenema, T. G., Thornton, C. P., Lavin, R. P., Bender, A. K., Seal, S., & Corley, A. (2017). Climate change–related water disasters' impact on population health. *Journal of Nursing Scholarship*, *49*(6), 625-634.

Velez, R., Calderon, D., Carey, L., Aime, C., Hultquist, C., Yetman, G., ... & Chen, R. S. (2022). Advancing Data for Street-Level Flood Vulnerability: Evaluation of Variables Extracted from Google Street View in Quito, Ecuador. *IEEE Open Journal of the Computer Society*, *3*, 51-61.

Verma, S., & Verma, R. K. (2023). SCS-CN methodology further modified. *Water Supply*, *23*(6), 2604-2622.

Viana, E. B., Galbetti, T. A. S., Galbetti, M. V., de Oliveira Ribeiro, V., & Diodato, J. O. (2022). Software para determinação de Chuvas de Projeto. *Terr@ Plural*, *16*, 1-12.

Vidal, X., Burgos, L., & Zevallos, O. (2018). 11 Protección y recuperación ambiental de las laderas del Pichincha en Quito, Ecuador. *Agua y Ciudades en América Latina*, 173.

Watson, C. S., Elliott, J. R., Ebmeier, S. K., Vásquez, M. A., Zapata, C., Bonilla-Bedoya, S., ... & Sevilla, E. (2022). Enhancing disaster risk resilience using greenspace in urbanising Quito, Ecuador. *Natural Hazards and Earth System Sciences*, *22*(5), 1699-1721.

Werner, M., Reggiani, P., Roo, A. D., Bates, P., & Sprokkereef, E. (2005). Flood forecasting and warning at the river basin and at the European scale. *Natural hazards*, *36*, 25-42.

Westra, S., Fowler, H. J., Evans, J. P., Alexander, L. V., Berg, P., Johnson, F., ... & Roberts, N. (2014). Future changes to the intensity and frequency of short-duration extreme rainfall. *Reviews of Geophysics*, *52*(3), 522-555.

Willkofer, F., Wood, R. R., & Ludwig, R. (2023). Assessing the impact of climate change on high return levels of peak flows in Bavaria applying the CRCM5 Large Ensemble. *EGUsphere*, *2023*, 1-31.

Wittemyer, G., Elsen, P., Bean, W. T., Burton, A. C. O., & Brashares, J. S. (2008). Accelerated human population growth at protected area edges. *Science*, *321*(5885), 123-126.

Zou, X. Y., Peng, X. Y., Zhao, X. X., & Chang, C. P. (2023). The impact of extreme weather events on water quality: International evidence. *Natural Hazards*, *115*(1), 1-21.